

Wavelet-based feature analysis of vehicle vibration signals for comfort assessment

Đorđe Damnjanović¹, Željko Jovanović¹, Marina Milošević¹, Nebojša Stanković¹, Nedeljko Dučić^{1*}

¹ University of Kragujevac, Faculty of Technical Sciences, Čačak, Serbia

ARTICLE INFO

* **Correspondence:** nedeljko.ducic@ftn.kg.ac.rs

DOI: 10.5937/engtoday2400002D

UDC: 621(497.11)

ISSN: 2812-9474

Article history: Received 11 April 2025; Revised 20 April 2025; Accepted 23 April 2025

ABSTRACT

This study explores the use of wavelet-based analysis for evaluating vehicle ride comfort through vibration signal processing. Using a custom-developed Android application, three-axis accelerometer and GPS data were collected under real driving conditions to identify three categories of passenger experience: comfortable, vibrationally uncomfortable, and oscillatory uncomfortable. The signals were decomposed using the Daubechies wavelet (Db2) up to level 8, and feature extraction was conducted using detail coefficients. Significant differences between signal types were observed through time and frequency domain analyses, with enhanced discrimination achieved via wavelet decomposition and RMS-based quantification. The results highlight that the vibrationally uncomfortable signals exhibit the highest coefficient values, clearly differentiating them from the other two categories. The findings confirm that wavelet-based methods provide improved insights into vibration signal characteristics, enabling more precise classification of discomfort. This work establishes a foundation for real-time comfort monitoring and future applications in transportation safety and healthcare, particularly in the context of patient transport.

KEYWORDS

Vehicle vibrations, Wavelet transform, Ride comfort, Vibration analysis, Detail coefficients, Android application, Feature extraction.

1. INTRODUCTION

Ride comfort is a critical factor in vehicle performance, affecting both passenger experience and vehicle design. Discomfort during rides has been extensively studied, with research covering road conditions, vehicle dynamics, human biomechanics, sensor technologies, and machine learning approaches. Whole-body vibration (WBV) is a primary contributor to ride discomfort [1], with higher frequency vibrations being associated with rough road conditions like bumps and potholes, while lower frequencies are known to cause motion sickness. The relationship between noise, vibration, and harshness (NVH) is also central to the design of modern vehicles [2], where optimizing vehicle noise and vibration characteristics, along with seat and suspension ergonomics, enhances overall ride quality [3], [4].

Advancements in sensor and smartphone technology have greatly improved the accuracy and cost-effectiveness of detecting sources of discomfort. Inertial measurement units (IMUs), gyroscopes, and GPS sensors are now widely used in vehicles and smartphones to monitor ride comfort [5] and real-time data processing in transportation and healthcare research [6]. They have been used to detect potholes based on vertical vibrations [7] and monitor traffic conditions using accelerometer and microphone data [8]. Additionally, wearable biomechanical sensors are being

employed to monitor passengers' physiological responses to vibrations, as highlighted in [9] and [10], underscoring the importance of reliable transport conditions for public health.

Suspension systems are a critical component in vehicle design, with optimized suspension designs improving both vehicle stability and passenger comfort by mitigating the effects of road-induced vibrations [3]. Furthermore, seat suspension systems have been shown to significantly affect ride comfort, with ergonomic designs providing greater comfort across different vehicle types [4].

The impact of road-induced vibrations extends beyond the vehicle itself, affecting the surrounding infrastructure. Studies show that rough road surfaces generate higher vibration levels, which are particularly problematic for heavy trucks operating on poorly maintained roads [11]. These vibrations can propagate through the ground and negatively affect nearby buildings, as discussed in [12].

In addition to affecting infrastructure, vibrations from road conditions also have significant health implications. Prolonged exposure to vehicle-induced vibrations has been linked to health problems, including musculoskeletal disorders, particularly in the lower back and spine [13]. The research in [14] emphasizes the adverse effects of automotive noise and vibrations on human health, while [15] explores the impact of road quality on bus drivers' exposure to WBV and the associated health risks. In the context of biomedical device diagnostics, study [16] demonstrate how vibration characteristics can improve the reliability of medical equipment.

In today's research, wavelets are rarely encountered in studies related to vehicle comfort or vehicle testing in general. Despite their primary purpose of improving certain properties of mathematical operations such as the Fourier transform [17], wavelets play a widespread role in feature extraction from various types of signals [18], [19]. The authors in [20], [21] focus on feature extraction from direct current motor signals, where differences between faulty and non-faulty motors can be successfully determined. The primary objective of this type of wavelet analysis is to decompose an audio signal into approximation and detail coefficients, but it can also be applied to other types of signals, as previously mentioned. This approach has been applied in many studies [22], [23], and detailed research has shown that wavelets can prepare features that can further be used for classification.

Vibrations are present in many fields, where wavelets find their application. The study [24] presents wavelet analysis as an alternative to classical Fourier Transform methods for signal processing, and that alternative is precisely wavelets. In the paper [25] authors examine vehicle vibrations on various road types, emphasizing the effectiveness of wavelet transform in detecting key signal features. By extracting crucial features from scalograms, the study aims to classify terrain and monitor road conditions in real-time, which can help optimize off-road vehicle performance. Study [26] explores the use of wavelets for fault diagnosis in the hydraulic brake system of a light motor vehicle, utilizing vibration signals obtained from a brake test setup with a piezoelectric accelerometer. This paper closely represents the research that lies ahead. In some studies, segmenting the signal into smaller frames before wavelet decomposition is desirable in order to achieve better results [21], [27], [28]. Such pre-processing of the signal is desirable when working with longer signals containing a larger number of samples, and segmentation is usually accompanied by frame overlap—most commonly 25%, 50%, or 75%. However, when dealing with shorter signals, as is the case in this study, segmentation can be omitted [27], especially if the decomposition process without segmentation yields satisfactory results.

This paper illustrates the application of wavelets to vehicle vibration signals in three different situations: when the travel is comfortable, when the travel is uncomfortably vibrating, and when the travel is uncomfortably oscillating. By applying wavelet decomposition and the Daubechies family of wavelets, features were obtained at 8 decomposition levels, which were thoroughly analyzed through their differences. The entire analysis process was conducted using the MATLAB software package. The paper is organized as follows: The introduction provides related work and an introduction to the study. The next section explains the Android application usage for transport comfort monitoring. The third section describes wavelets and their decomposition into approximation and detail coefficients mathematically. The results are then presented. The conclusion outlines certain observations from the study and provides directions for future work.

2. ANDROID APPLICATION USAGE FOR TRANSPORT COMFORT MONITORING

An Android application was developed to monitor passenger transport comfort using data from a three-axis accelerometer and GPS sensor. The application begins by calibrating the accelerometer axes: The Z-axis represents the movement direction, the X-axis corresponds to lateral movement, and the Y-axis represents vertical movement. This calibration allows for a detailed analysis of discomfort caused by assessing acceleration values across all axes.

The application operates using separate threads for accelerometer and GPS monitoring, implemented with RxJava [29]. Once the parameters are set, the accelerometer and GPS data collection begin. The application continuously plots real-time accelerometer signals on the phone display while performing comfort calculations. Each driving ses-

sion is divided into 10-second intervals, balancing real-time accuracy with practical monitoring. Shorter intervals (e.g., 5 seconds) were tested but led to higher data variability, while longer intervals (e.g., 15 seconds) risked overlooking brief discomfort events. User feedback and additional tests confirmed that a 10-second interval provides optimal accuracy and usability. The use of a three-axis accelerometer enhances accuracy by capturing the full range of vehicle vibrations compared to traditional single-axis measurements. The phone was placed inside a vehicle, which is presented in Figure 1 a) with red rectangle, and axis orientation are presented in Figure 1. b). This location captures signals from the middle of the vehicle, between the driver and a passenger, so important vibrations felt from both sides of the vehicle are detected.



Figure 1: a) Android application usage, b) axis orientation

3. WAVELETS

Wavelets are essential mathematical tools for analyzing and processing signals and images. In signal analysis, they allow for the representation and interpretation of complex signals using localized functions that vary in time or frequency. This technique enables the efficient detection and analysis of various signal properties, such as frequency, amplitude, or shape changes [30].

The key advantage of wavelets, compared to traditional methods like Fourier transforms, lies in their superior ability to localize both time and frequency. This feature is particularly beneficial for analyzing rapidly changing signals or images with different levels of detail. By employing wavelets, it's possible to conduct multi-scale analysis, which enhances pattern recognition and feature extraction for signals. At its core, a wavelet is a wave-like function of finite duration with a zero average value. These wavelets have been developed to improve existing signal processing algorithms and overcome certain limitations of traditional methods. The basic wavelet, known as the "mother wavelet" $\psi(x)$, is defined as [30], [31]:

$$\psi_{a,b}(x) = \frac{1}{\sqrt{a}} \psi\left(\frac{x-b}{a}\right), a > 0 \quad (1)$$

where a is the scaling parameter and b is the translation parameter. Choosing the appropriate parameters is one of the most challenging aspects of wavelet functions, as it depends on the shape and complexity of the wavelet.

All wavelet transformations can be viewed as time-frequency representations for continuous (analog) signals, making them analogous to harmonic analysis. The Continuous Wavelet Transform (CWT) utilizes wavelets that allow for signal analysis in continuous time, breaking down the signal into localized functions in both time and frequency domains. This technique is similar to Fourier analysis, but it provides improved time-frequency localization. The CWT is defined by the inner product of a function (f) and the basis "mother" wavelet $\psi_{a,b}(x)$ [30], [31]:

$$CWT_f(a,b) = (f, \psi_{a,b}) = \frac{1}{\sqrt{a}} \int_{-\infty}^{\infty} f(x) \psi^*\left(\frac{x-b}{a}\right) dx \quad (2)$$

For the purpose of feature extraction from signals, the most commonly used method involving wavelets is the discrete wavelet transform. This method relies on signal decomposition using wavelets, where approximation and detail coefficients are formed. First, it is important to consider how the discrete wavelet transform is obtained. The following expression is represented by the next formula [32]:

$$\psi_{i,j}(x) = \frac{1}{\sqrt{a_0^i}} \psi\left(\frac{x - ja_0^i b_0}{a_0^i}\right) = a_0^{-i/2} \psi(a_0^{-i} x - jb_0), a_0 > 0 \quad (3)$$

where a_0 and b_0 are the scale and time steps, respectively, and i and j are integers. The steps a_0 and b_0 determine the scaling and translation of the wavelet along the signal. Compared to equation (1), a_0 and b_0 can be expressed through following formulas: $a = a_0^i$ and $b = ja_0^i b_0$.

The previously defined functions also represent one of the most important characteristics of the discrete wavelet transform, namely the decomposition into levels, where at each level of decomposition, the detail and approximation coefficients are calculated. At each level of decomposition, the signal is filtered using a high-pass filter (HPF) and a low-pass filter (LPF) [21], [30]. The outputs from the filters are passed into a downsampling block, which performs downsampling of the signal at a lower sampling frequency than usual, in this case, the factor is 2. This means that at each level of decomposition, detail coefficients (D) and approximation coefficients (A) are obtained, with half the number of coefficients compared to the previous level. The process for approximation coefficients is repeated until the final level of decomposition, where the obtained approximation coefficients are passed through the HPF and LPF filters at each subsequent level, followed by downsampling, and so on until the final level. The whole process is presented in Figure 2, where decomposition levels go to 4.

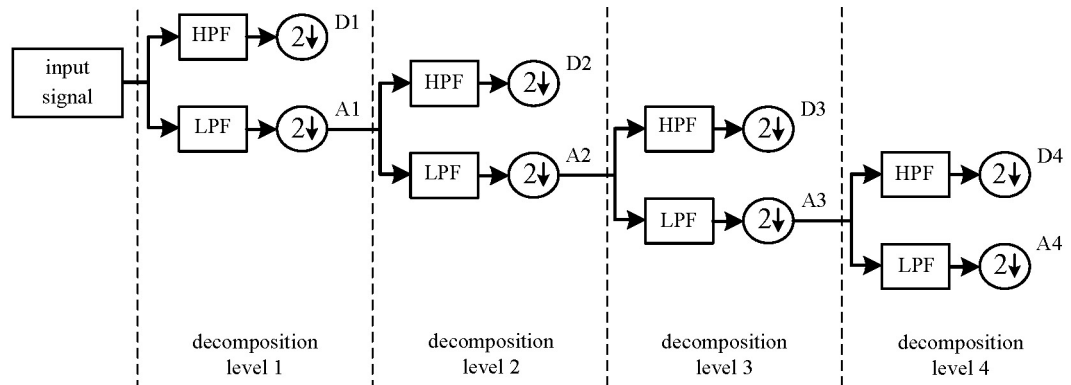


Figure 2: Block diagram of wavelet transform decomposition into detail and approximation coefficients

Currently, various types of wavelets are used across different fields of signal analysis, image processing, and mathematics. Some of the most widely recognized wavelets include Haar, Daubechies, Coiflets, Symlet, Biorthogonal, Reverse Biorthogonal, Meyer, and Morlet, among others.

4. RESULTS OF APPLYING WAVELETS

As previously explained, the results of vehicle comfort signal processing in this study are classified into three categories: comfortable, vibrationally uncomfortable, and oscillatory uncomfortable. The analysis of these signals begins with their representation in the time and frequency domains. Figure 3 represents all three signals in time domain. It is important to emphasize that all three presented signals represent the modulus of all three axes, preceded by high-pass filtering of each axis individually.

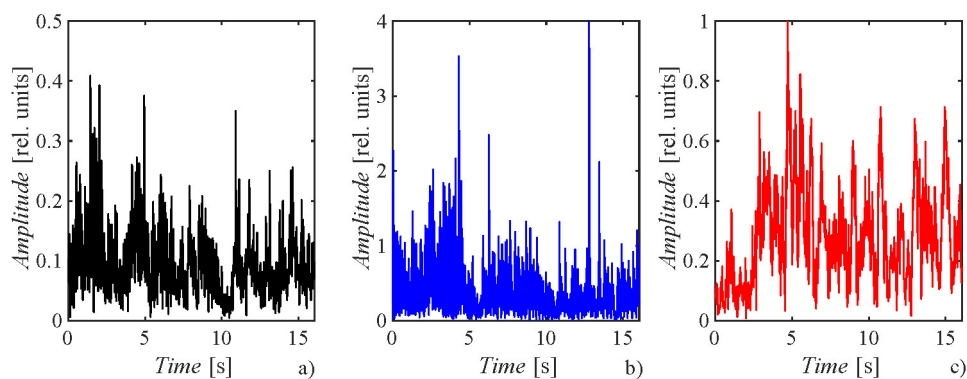


Figure 3: Time domain of the vehicle comfort signal:
 a) comfortable, b) vibrationally uncomfortable, c) oscillatory uncomfortable

As can be seen from the previous image, the amplitudes of the signals vary significantly. The signal representing comfortable driving has the smallest amplitude, which is expected. The signal representing constant vibrations in uncomfortable driving has the largest amplitude. The amplitude spectra of the mentioned signals are shown in Figure 4. The impact of amplitude can be observed here as well, and it matches the analysis in the time domain. However, for a deeper discussion, it would be necessary to use a different model, such as a spectrogram or scalogram.

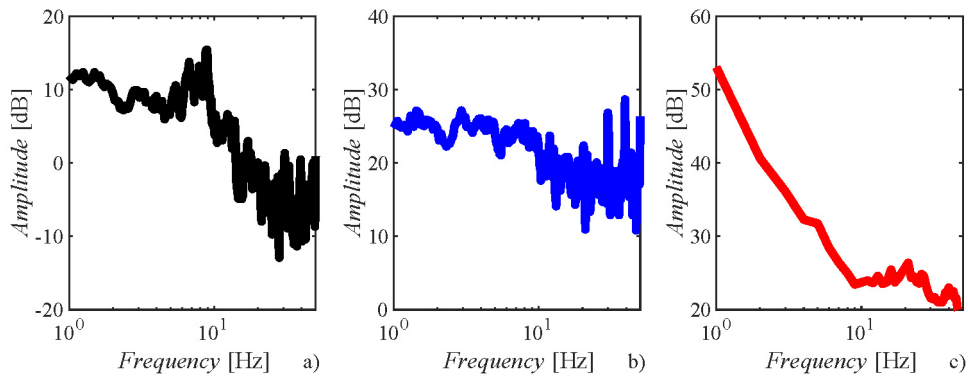


Figure 4: Frequency domain of the vehicle comfort signal:
 a) comfortable, b) vibrationally uncomfortable, c) oscillatory uncomfortable

Since wavelet analysis itself is expressed through frequency content, we will also focus on comparing the obtained spectra when all are shown on the same graph. Figure 5 represents all the amplitude spectra of the analyzed signals on the same plot. In all subsequent results, abbreviations will be used for the mentioned signals in Figures and tables: COM for the comfortable signal, VUCOM for the vibrating uncomfortable signal, and OUCOM for the oscillatory uncomfortable signal.

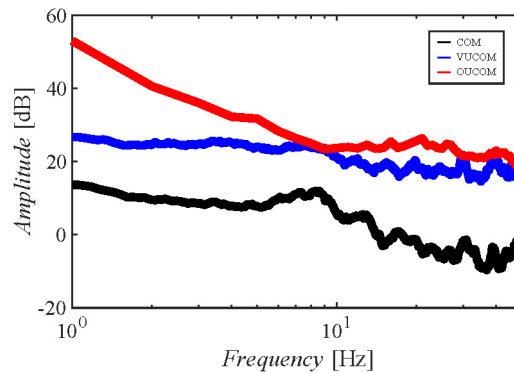


Figure 5: Frequency domain of all 3 vehicle comfort signals

The previously described analysis in the frequency domain of the individual signal is now shown in Figure 5. It should again be noted, considering the impact of the signal's amplitude, that the signal during comfortable driving has the least influence (black graph in Figure 5).

4.1. Wavelet decomposition

After the initial analysis in the time and frequency domains, the previously described signals are now decomposed into 8 levels using wavelets, with the focus on the detail coefficients at each level (see Figure 6). In this case, 8 levels of decomposition were chosen because at the last 8th level, the number of detail coefficients is very small, and further decomposition would lead to information that would not be of significant importance [21]. Decomposition and determination of detail coefficients is precisely the feature analysis in the frequency domain that characterizes wavelets. In all subsequent result presentations, the Daubechies 2 wavelet was used, as previously mentioned.

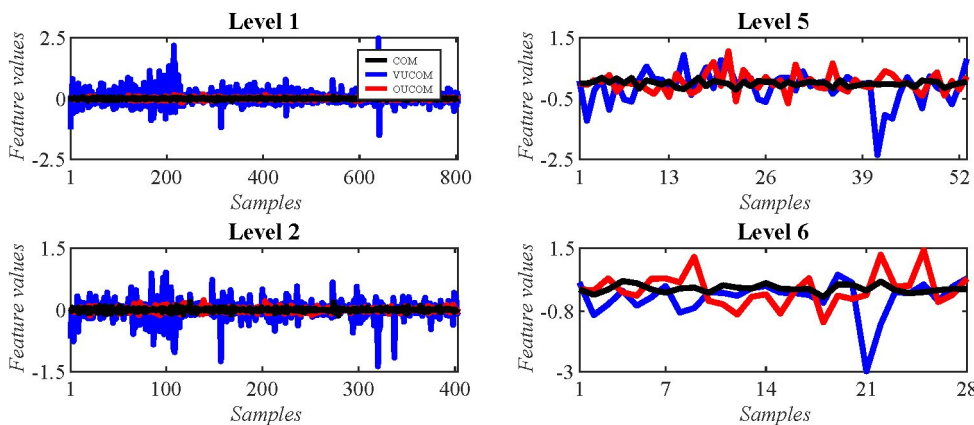


Figure 6: Detail coefficients after applying Daubechies 2 wavelet to the vehicle comfort signals

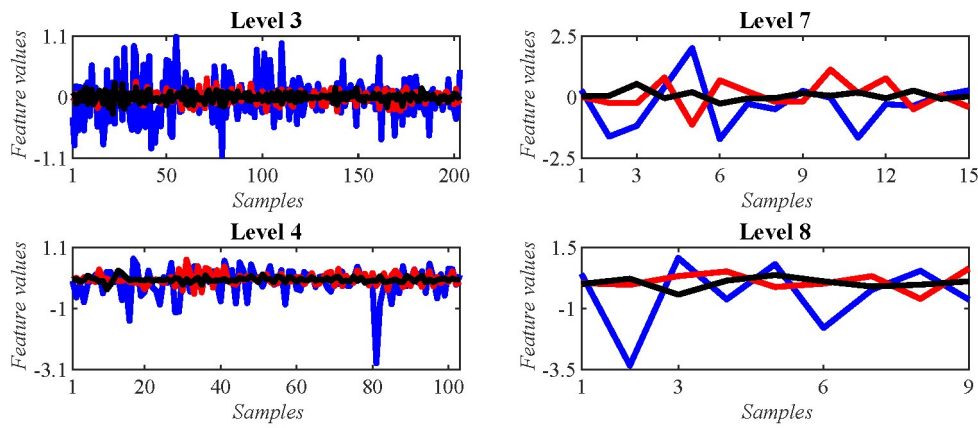


Figure 6: Detail coefficients after applying Daubechies 2 wavelet to the vehicle comfort signals

Observing Figure 6, the extracted features differ to some extent, meaning that the detail coefficients have provided a certain result that indicates the need for further analysis. The vibrating uncomfortable signal exhibits the most distinct features, which, at almost every level of decomposition, differ to some degree from the other two signals. Although the spectrum did not fully reveal this situation, wavelets allow for a deeper analysis, making the feature extraction method using detail coefficients a more advanced approach in many cases.

The coefficients obtained from the oscillatory uncomfortable signal differ slightly from those of the comfortable signal. However, at certain decomposition levels, this difference becomes quite noticeable—for example, at level 6 (see Figure 6). This indicates that the analysis should be further deepened using specific methods to achieve better results and conclusions. To confirm these previous considerations and determine whether there are differences in the extracted features values, the absolute value will be applied at each decomposition level for all three signals. The result of this analysis is shown in Figure 7.

What has been proven is that the vibrating uncomfortable signal remains significantly different from the other two signals even after calculating the absolute values of the detail coefficients. At any level of decomposition, the difference is evident. However, when observing the oscillatory uncomfortable signal and the comfortable signal, greater differences now appear at certain decomposition levels. In addition to level 6, levels 4, 5, and 7 can also be distinguished, which represents a significant improvement compared to the analysis without absolute values.

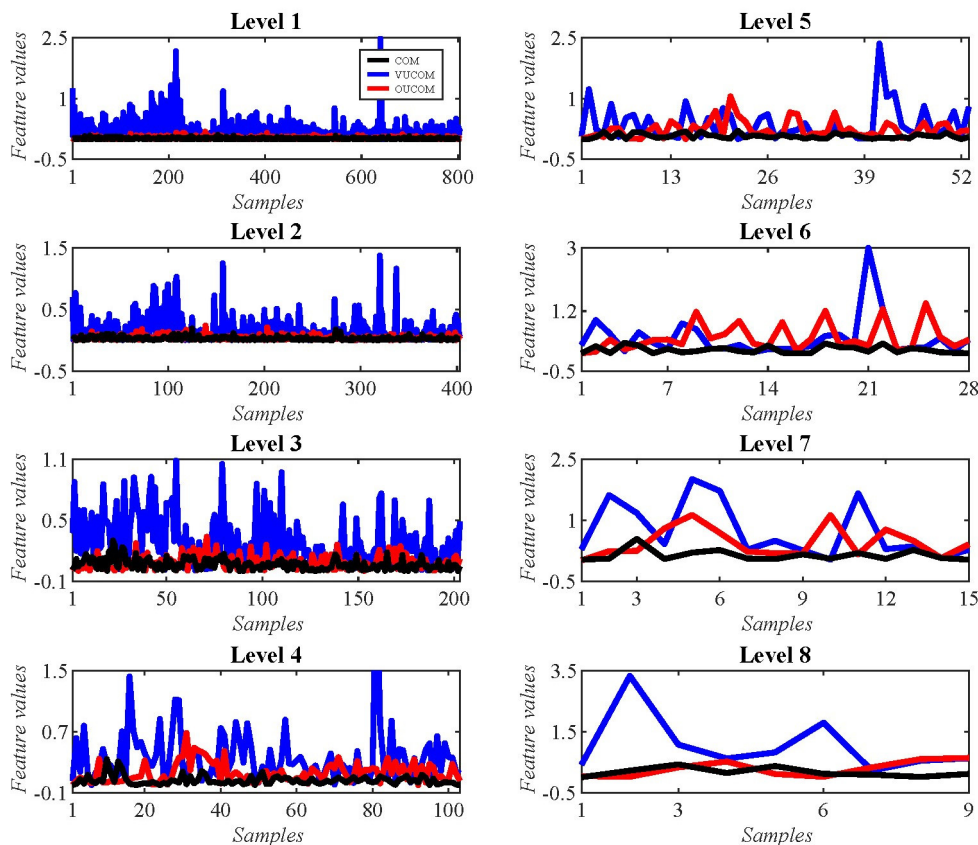


Figure 7: Absolute values of detail coefficients after applying Daubechies 2 wavelet to the vehicle comfort signals

4.2. Highlighted cases and numerical differences

The following analysis will focus on selected cases and the discussion related to them. To gain a closer insight into the detail coefficients of the chosen signals after wavelet processing, two signals will be compared instead of three in certain selected cases. The numerical value at each level of decomposition will also be determined in the form of the root mean square (RMS), and all signal values will be presented in a table to compare the observed differences. The comfortable signal will serve as the reference signal in the initial selected comparisons, but in the final analysis, the vibrating uncomfortable and the oscillatory uncomfortable signals will also be compared. For the results in this subsection, the absolute value of the detail coefficients will be used, as was the case in Figure 7. The following analysis presents a comparison between the comfortable signal and the vibrating uncomfortable signal. Three specific cases are highlighted at decomposition levels 1, 3, and 8 (see Figure 8). It can be immediately concluded that the difference in detail coefficients between these two signals is significant, which was also anticipated in the previous analysis.

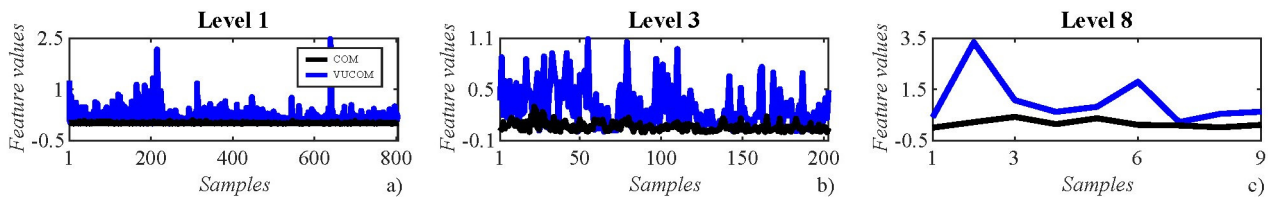


Figure 8: Absolute values of detail coefficients after applying Daubechies 2 wavelet to the comfortable signal and the vibrating uncomfortable signal at the decomposition level: a) 1, b) 3, c) 8

The next case compares the comfortable signal with the oscillatory uncomfortable signal (Figure 9). The selected cases are at decomposition levels 4, 6, and 7. The differences in detail coefficients are smaller but still noticeable, revealing characteristics that could be useful for future classification.

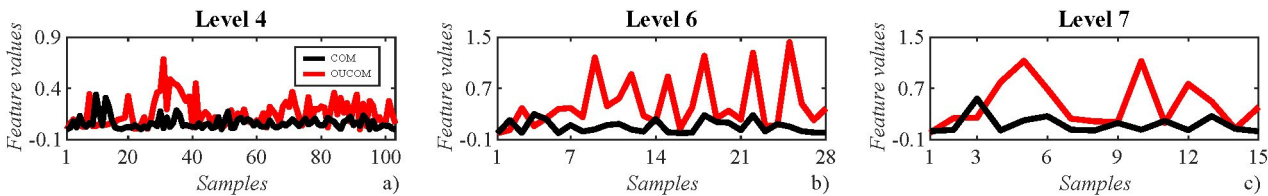


Figure 9: Absolute values of detail coefficients after applying Daubechies 2 wavelet to the comfortable signal and the oscillatory uncomfortable signal at the decomposition level: a) 4, b) 6, c) 7

The final case presented in Figure 10 compares the vibrating, uncomfortable signal with the oscillatory, uncomfortable signal. A significant observation is that the differences between these two signals are clearly noticeable, suggesting that this case could also be considered in further analysis. This implies that the comfortable signal may not always need to be used as a reference in certain cases. Regarding decomposition levels, the detail coefficients are shown at levels 1, 3, and 8.

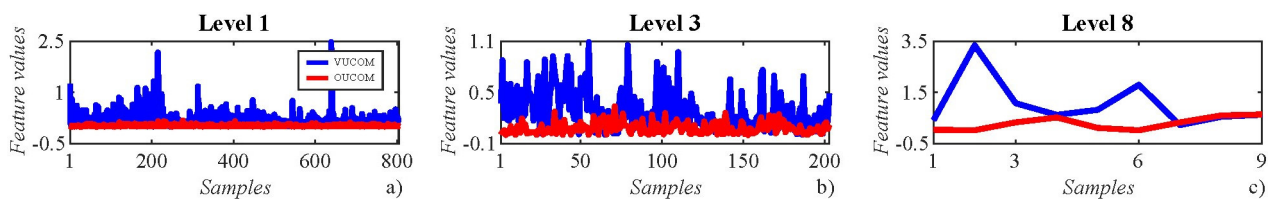


Figure 10: Absolute values of detail coefficients after applying Daubechies 2 wavelet to the vibrating uncomfortable signal and the oscillatory uncomfortable signal at the decomposition level: a) 1, b) 3, c) 8

For a more detailed analysis of the previous results, two tables are provided below. Table 1 presents the values of detail coefficients at each level using the RMS method. This method was applied to the detail coefficients shown in the Figure 7, where the absolute value of each coefficient was used beforehand. Analyzing the results from Table 1, it can be observed that the RMS values of the vibrating uncomfortable signal are the highest, while those of the comfortable signal are the lowest. The values of the oscillatory uncomfortable signal are, in some cases, almost identical to those of the comfortable signal, but at certain levels, the RMS values differ significantly. All these observations confirm the previously stated findings and graphical analyses.

Table 1: Root mean square values of the vehicle comfort signals at each decomposition level

Vehicle comfort signals	Level 1	Level 2	Level 3	Level 4	Level 5	Level 6	Level 7	Level 8
COM	0.02	0.04	0.08	0.09	0.09	0.14	0.19	0.22
VUCOM	0.30	0.26	0.38	0.52	0.56	0.72	0.99	1.4
OUCOM	0.04	0.05	0.11	0.21	0.32	0.60	0.57	0.38

Table 2 presents an additional analysis highlighting the differences between the RMS values shown in Table 1. The first row displays the differences between the vibrating uncomfortable signal and the comfortable signal, the second row shows the differences between the oscillatory, uncomfortable signal and the comfortable signal, and the third row presents the differences between the vibrating uncomfortable signal and the oscillatory uncomfortable signal.

It is important to emphasize that all obtained results are positive, which supports the previous claims that the vibrating uncomfortable signal produces the highest amplitudes in the coefficients and results in the largest values, the oscillatory uncomfortable signal ranks second, while the comfortable signal has the lowest values, as demonstrated in the previous analyses.

Table 2: Root mean square differences between the vehicle comfort signals at each decomposition level

Vehicle comfort signals	Level 1	Level 2	Level 3	Level 4	Level 5	Level 6	Level 7	Level 8
VUCOM – COM	0.28	0.22	0.30	0.43	0.47	0.58	0.80	1.18
OUCOM – COM	0.02	0.01	0.03	0.12	0.23	0.46	0.38	0.16
VUCOM – OUCOM	0.26	0.21	0.27	0.31	0.24	0.12	0.42	1.02

All obtained results, both graphical and numerical, demonstrate significant differences in detail coefficients when applying wavelets to signals measured during vehicle rides under different conditions. It is important to emphasize that these results were selected from a large number of samples and that this analysis could be further enriched with many additional examples.

Furthermore, these three types of signals are not the only cases that occur during driving; future research should also consider analyzing other scenarios. It should also be noted that this study serves as a preliminary analysis of signal features using wavelets, which can later be applied to a classification process.

5. CONCLUSION

Poor road conditions generally cause significant discomfort during driving, especially when transporting patients in hospital vehicles. Consequently, ride analysis can help improve vehicle comfort on such roads.

Previous studies have shown that multiple criteria define the types of discomfort caused by potholes, uneven surfaces, poor pavement quality, and other factors. However, it is also essential to consider that the vehicle's quality itself can contribute to an uncomfortable ride.

This study presented the application of wavelets in analyzing the characteristics of measured vehicle comfort signals under three different driving conditions. The first and fundamental, or reference, signal represents a comfortable ride—when there are no road irregularities and the vehicle is assumed to be mechanically sound. The second type of recorded and analyzed signal corresponds to constant vibrations during driving, typically occurring on uneven roads, such as gravel or secondary roads instead of smooth asphalt. The third type of signal represents oscillations during driving—rocking motions caused by frequent curves in the road, which can further induce nausea, especially in the case of patient transportation.

The Daubechies wavelet (Db2) was applied to all three types of signals with a decomposition level of 8. A high-pass filter was used on all signals. The signals were recorded along three axes, but in the final analysis, the modulus of all three axes was used for each signal. The extracted features were represented through detail coefficients at each decomposition level, where the coefficients of all three signals were compared to identify specific differences for future classification. The initial analysis immediately revealed certain results and noticeable differences between the coefficients. However, applying the absolute value to all coefficients clarified the overall picture, offering a stronger basis for further analysis. The graphical results clearly show that the largest differences occur between the comfortable signal and the vibrating uncomfortable signal, as well as between the vibrating uncomfortable signal and the oscillatory uncomfortable signal. The differences between the comfortable signal and the oscillatory uncomfortable signal are significantly smaller. However, at certain decomposition levels, they are still present to a degree that cannot be ignored. The results achieved in this study using Db2 wavelets were more than satisfactory. The entire process could have been extended to other wavelet families as well, but due to space limitations, those results are not presented here. A clear indication of the usefulness of this analysis is that these results can be further utilized in other methods, which were less effective in providing significant insights compared to the wavelet-based approach.

It should be noted that, in addition to graphical representations, this study also involved calculating the RMS values of the detail coefficients for each signal at every decomposition level. This method was applied to validate the graphical results. Finally, the differences between the RMS values of all three signals were calculated, ultimately demonstrating that the comfortable ride signal had the lowest detail coefficient values, i.e., the lowest RMS values. The most influential signal in terms of magnitude was the vibrating uncomfortable signal, as indicated by the coefficients obtained after wavelet analysis.

Future research will focus on recording a larger number of signals, creating a database of these signals, and analyzing them using all the mentioned methods. Additionally, it will explore different wavelet families and decomposition levels. Ultimately, all collected features should be utilized for some form of classification. It might also be valuable to analyze each axis of the recorded signals separately and provide specific recommendations for recognition and future classification.

ACKNOWLEDGEMENTS

This research has been supported by the research grants of the Serbian Ministry of Science, Technological Development and Innovations, grant No. 451-03-136/2025-03/ 200132 with University of Kragujevac – Faculty of Technical Sciences Čačak.

REFERENCES

- [1] Mechanical vibration and shock -- Evaluation of human exposure to whole-body vibration -- Part 1: General requirements, ISO Standard 2631-1, (1997)
- [2] D. Song, S. Hong, J. Seo, K. Lee, and Y. Song, "Correlation analysis of noise, vibration, and harshness in a vehicle using driving data based on big data analysis technique", *Sensors*, Vol. 22(6), p. 2226, <https://doi.org/10.3390/s22062226>, (2022)
- [3] R. Wang, W. Liu, R. Ding, X. Meng, Z. Sun, L. Yang, and D. Sun, "Switching control of semi-active suspension based on road profile estimation," *Vehicle System Dynamics*, Vol. 60(6), pp. 1972-1992, <https://doi.org/10.1080/00423114.2021.1889621>, (2022)
- [4] A. Heidarian and X. Wang, "Review on seat suspension system technology development", *Applied Sciences*, Vol. 9(14), p. 2834, <https://doi.org/10.3390/app9142834>, (2019)
- [5] K. Lee and M-P. Kwan, "Automatic physical activity and in-vehicle status classification based on GPS and accelerometer data: A hierarchical classification approach using machine learning techniques", *Transactions in GIS*, Vol. 22(6), pp. 1522-1549, <https://doi.org/10.1111/tgis.12485>, (2018)
- [6] S. R. Steinhubl, E. D. Muse, and E. J. Topol, "The emerging field of mobile health", *Science Translational Medicine*, Vol. 7(283), p. 283rv3, <https://doi.org/10.1126/scitranslmed.aaa3487>, (2015)
- [7] A. Mednis, G. Strazdins, R. Zviedris, G. Kanonirs, and L. Selavo, "Real time pothole detection using Android smartphones with accelerometers", 2011 International Conference on Distributed Computing in Sensor Systems and Workshops (DCOSS'11), Barcelona (Spain), pp. 1-6, <https://doi.org/10.1109/DCOSS.2011.5982206>, (2011)
- [8] P. Mohan, V. N. Padmanabhan, and R. Ramjee, "TrafficSense: Rich monitoring of road and traffic conditions using mobile smartphones", Microsoft Research Technical Report MSR-TR-2008-59, The 6th ACM Conference on Embedded Networked Sensor Systems, pp. 1–29, (2008)
- [9] S. Zhang, X. Lin, J. Wan, C. Xu, and M. Han, "Recent progress in wearable self-powered biomechanical sensors: mechanisms and applications", *Advanced Materials Technologies*, Vol. 9(21), p. 2301895, <https://doi.org/10.1002/admt.202301895>, (2024)
- [10] N. Mallegni, G. Molinari, C. Ricci, A. Lazzeri, D. La Rossa, A. Crivello, and M. Milazzo, "Sensing devices for detecting and processing acoustic signals in healthcare", *Biosensors*, Vol. 12(10), p. 835, <https://doi.org/10.3390/bios12100835>, (2022)
- [11] R. Zhou, L. Yan, B. Li, and J. Xie, "Measurement of truck transport vibration levels in China as a function of road conditions, truck speed and load level", *Packaging Technology and Science*, Vol. 28(11), pp. 949-957, <https://doi.org/10.1002/pts.2176>, (2015)
- [12] O. O. Ajayi, M. C. Agarana, I. I. Akinwumi, P. I. Okokpujie, E. Y. Salawu, A. A. Abioye, A. S. Afolalu, and R. O. Leramo, "Modelling rate of traffic-induced building vibrations in Sango-Ota, Nigeria: An assumption based analysis", *WIT Transactions on the Built Environment*, Vol. 182, pp. 303-313, <https://doi.org/10.2495/ut18028>, (2019)
- [13] L. Schneider, D. Sogemeier, T. Jaitner, A. Buchner, and N. Stutzig, "Adaptions in back muscle activity in long-haul truck drivers during prolonged driving with and without seat-integrated stimulation", *International Journal of Industrial Ergonomics*, Vol. 96, p. 103475, <https://doi.org/10.1016/j.ergon.2023.103475>, (2023)
- [14] M. Ratiu, M. A. Prichici, A. Rus, S. Bogdan, and M. B. Tataru, "Study on the impact of automotive noise and vibration on human health and environment", *Preprints*, <https://doi.org/10.20944/preprints202311.1003.v1>, (2023)
- [15] G. Wang, J. Zhang, and X. Kong, "Study on passenger comfort based on human-bus-road coupled vibration", *Applied Sciences*, Vol. 10(9), p. 3254, <https://doi.org/10.3390/app10093254>, (2020)

- [16] W. Mohamedi, "Application of vibration analysis for medical diagnosis", *Progress in Medical Devices*, Vol. 2(1), pp. 12-18, <https://doi.org/10.61189/581835yrfifv>, (2024)
- [17] M. Sifuzzaman, M. R. Islam, and M. Z. Ali, "Application of wavelet transform and its advantages compared to Fourier transform", *Journal of Physical Sciences*, Vol. 13, pp. 121-134, (2009)
- [18] G. Tzanetakis, G. Essl, and P. R. Cook, "Audio analysis using the discrete wavelet transform", *Proceedings of the WSES International Conference Acoustics and Music: Theory and Applications (AMTA 2001)*, Skiathos (Greece), pp. 318-323, (2001)
- [19] M. Zhao, Q. Chai, and S. Zhang, "A method of image feature extraction using wavelet transforms", *Proceedings of the 5th International Conference on Intelligent Computing*, Ulsan (South Korea), pp. 187-192, https://doi.org/10.1007/978-3-642-04070-2_21, (2009)
- [20] Đ. Damjanović, D. Ćirić, and D. Vujičić, "Analysis for industrial product sounds by using discrete Meyer wavelet", *Proceedings of the 9th International Conference on Electrical, Electronic and Computing Engineering "IcETRAN 2022"*, Novi Pazar (Serbia), pp. 12-17, (2022)
- [21] Đ. Damjanović, D. Ćirić, and Z. Perić, "Wavelet-based audio features of DC motor sound", *Facta universitatis - series: Electronics and Energetics*, Vol. 34(1), pp. 71-88, <https://doi.org/10.2298/FUEE2101071D>, (2021)
- [22] C. da Costa, M. Kashiwagi, and M. H. Mathias, "Rotor failure detection of induction motors by wavelet transform and Fourier transform in non-stationary condition", *Case Studies in Mechanical Systems and Signal Processing*, Vol. 1, pp. 15-26, <https://doi.org/10.1016/j.csmssp.2015.05.001>, (2015)
- [23] P. Sharma and N. Saraswat, "Diagnosis of motor faults using sound signature analysis", *International Journal of Innovative Research in Electrical, Electronics, Instrumentation and Control Engineering*, Vol. 3(5), pp. 80-83, (2015)
- [24] T. Kaynaş and S. Şeker, "Wavelet Analysis for Vibration Signals," *Istanbul University - Journal of Electrical & Electronics Engineering*, Vol. 8(1), pp. 581-584, (2008)
- [25] M. Vlkovský, P. Koziol, and D. Grzesica, "Wavelet based analysis of truck vibrations during off-road transportation", *MATEC Web of Conferences*, Vol. 211, 11009, <https://doi.org/10.1051/mateconf/201821111009>, (2018)
- [26] T. M. Alamelu Manghai and R. Jegadeeshwaran, "Vibration based brake health monitoring using wavelet features: A machine learning approach", *Journal of Vibration and Control*, Vol. 25(18), pp. 2534-2550, <https://doi.org/10.1177/1077546319859704>, (2019)
- [27] R. S. S. Kumari and D. Sugumar, "Wavelet based feature vector formation for audio signal classification", *Proceedings of the ICACC2007 International Conference*, Madurai (India), pp. 752-755, (2007)
- [28] A. Glowacz, "Diagnostics of direct current machine based on analysis of acoustic signals with the use of symlet wavelet transform and modified classifier based on words", *Eksplotacja i Niezawodność – Maintenance and Reliability*, Vol. 16(4), pp. 554-558, (2014)
- [29] A. L. Davis, "Android and RxJava", in: *Reactive Streams in Java*, Apress, Berkeley, California (USA), https://doi.org/10.1007/978-1-4842-4176-9_7, (2019)
- [30] R. J. E. Merry, "Wavelet Theory and Applications: A literature study", in: *DCT rapporten*, Vol. 2005.053, Technische Universiteit Eindhoven, (2005)
- [31] B. Ergen, "Signal and image denoising using wavelet transform", in: *Advances in Wavelet Theory and Their Applications in Engineering, Physics and Technology*, pp. 495-514, <https://doi.org/10.5772/2668>, (2012)
- [32] M. Y. Gokhale and D. K. Khanduja, "Time domain signal analysis using wavelet packet decomposition approach", *International Journal of Communications, Network and System Sciences*, Vol. 3, pp. 321-329, <http://dx.doi.org/10.4236/ijcns.2010.33041>, (2010)